ECOLOGY

Population-specific vulnerability to ocean change in a multistressor environment

Emily M. Donham[1]*†, Iris Flores[1], Alexis Hooper[1], Evan O'Brien[1], Kate Vylet[2], Yuichiro Takeshita[3], Jan Freiwald[2,4], Kristy J. Kroeker[1]*

Variation in environmental conditions across a species' range can alter their responses to environmental change through local adaptation and acclimation. Evolutionary responses, however, may be challenged in ecosystems with tightly coupled environmental conditions, where changes in the covariance of environmental factors may make it more difficult for species to adapt to global change. Here, we conduct a 3-month-long mesocosm experiment and find evidence for local adaptation/acclimation in populations of red sea urchins, *Mesocentrotus franciscanus*, to multiple environmental drivers. Moreover, populations differ in their response to projected concurrent changes in pH, temperature, and dissolved oxygen. Our results highlight the potential for local adaptation/acclimation to multivariate environmental regimes but suggest that thresholds in responses to a single environmental variable, such as temperature, may be more important than changes to environmental covariance. Therefore, identifying physiological thresholds in key environmental drivers may be particularly useful for preserving biodiversity and ecosystem functioning.

INTRODUCTION

Global climate change is occurring at an unprecedented rate due to anthropogenic activities. Our current understanding of how climate change will affect species and ecosystems is largely based on studies conducted on a single population of a target species or community, yet local adaptation and phenotypic plasticity can substantially alter how species respond to environmental change (*1*). Increasingly, studies focused on evolutionary rescue are providing insights into the mechanistic underpinnings of intraspecific variability in response to changes in a single environmental driver [e.g., temperature (*2*) and acidification (*3*–*8*); but see (*9*)]. The environmental conditions that organisms experience are, however, inherently multivariate, and global change is expected to alter multiple environmental drivers simultaneously. Understanding the potential for species to adapt to multivariate environmental change is a key unanswered question.

Adaptation in the face of multiple environmental changes may be especially complex because of species' underlying genetic architecture. For instance, pleiotropy can limit adaptation when selection on different traits controlled by the same gene is opposing (*10*). This may occur more frequently in environments where multiple abiotic drivers influence fitness, if the number of traits under selection increases with the number of abiotic drivers (*11*). Furthermore, in addition to a single gene influencing multiple traits, a single trait can be influenced by multiple genes [i.e., polygenic traits (*12*)], and in some cases, different genes can even produce the same phenotype (*13*). Polygenic traits have been shown to be important for tolerance to temperature (*13*, *14*), hypoxia (*14*), pH (*4*), and pH and temperature (*15*). Genetic redundancy in polygenic traits may be especially important in multivariate environments since multiple pathways can lead to the same phenotypic outcomes, allowing for more genetic flexibility. In addition to the importance of pleiotropy and polygenic traits in shaping species' adaptive responses to global change, increases in the strength of selection may become more likely as the number of environmental drivers increases (*11*). Increased selection intensity could either lead to rapid adaptive evolution or further constrain adaptive evolution through reductions in population size, which may prove detrimental if large populations are necessary to maintain rare beneficial alleles (*4*). Although it is crucial to improve our mechanistic understanding of species' adaptive responses (i.e., genetic changes), measurements of intraspecific variation in traits (due to adaptation, acclimation, or plasticity) across different populations provide critical, first-order information about a species' capacity to adapt to multivariate change.

Recent work (*16*) has shown that understanding a species' response to a single dominant environmental driver may be particularly useful in predicting species' responses to changes in multiple environmental drivers. Although this approach may prove useful in some systems, it may also be less accurate in tightly coupled multivariate environments where organisms are prepared for specific covarying conditions that influence physiological responses. For instance, a species' stress response to one environmental driver can prime an individual for exposure to a second environmental driver due to shared signal pathways (cross-talk) or protective mechanisms (cross-tolerance) (*17*). If the environmental signals change rapidly and/or in opposing directions, cross-talk or cross-tolerance mechanisms could become ineffective or even an unnecessary expense. However, there is some evidence that mechanisms to cope with simultaneous changes in multiple stressors may be more general (e.g., heat shock proteins, antioxidants, and detoxification enzymes) and therefore could be advantageous regardless of the identity of any specific environmental factor (*18*). Further insights into the relative importance of dominant drivers versus changes to covariance in multiple drivers in shaping species

[1]Department of Ecology and Evolutionary Biology, University of California, Santa Cruz, Santa Cruz, CA 95064, USA. [2]Reef Check Foundation, Marina del Rey, CA 90929, USA. [3]Monterey Bay Aquarium Research Institute, Moss Landing, CA 95039, USA. [4]Institute of Marine Sciences, University of California, Santa Cruz, Santa Cruz, CA 95064, USA.
*Corresponding author. Email: edonham@ucsc.edu (E.M.D.); kkroeker@ucsc.edu (K.J.K.)
†Present address: Department of Ecology, Evolution, and Marine Biology, University of California, Santa Barbara, Santa Barbara, CA 93106, USA.

responses will be crucial to improving our ability to predict future ecological change.

Because of the relatively recent technological advances that facilitate high-resolution measurements of oceanographic conditions [e.g., pH and dissolved oxygen (DO)], there is increasing recognition that small-scale variation in a broad range of environmental drivers can lead to local adaptation and acclimation of marine organisms (*19*). Within eastern boundary upwelling systems, marine species experience dynamic oceanographic conditions that vary both spatially and temporally (*20*–*22*). During seasonal upwelling events, cold waters that are reduced in pH and DO are brought to the surface. Differences in the strength and magnitude of upwelling create a persistent mosaic of environmental conditions at small spatial scales (*21*, *23*). For example, in the California Current System (CCS), northern and central California experience more frequent and intense upwelling compared to southern California, although "shadow zones" of less intense upwelling also occur within these regions (*24*). There is emerging evidence for local selection (which could lead to local adaptation) under exposure to environmental conditions associated with upwelling within the CCS, including species with high pelagic larval durations (*4*–*7*, *25*–*27*). It is still unclear, however, whether local adaptation/acclimation confers greater resilience to future changes in both the mean and covariance in multiple environmental variables.

Climate change and ocean acidification (OA) are expected to progress rapidly in the CCS, resulting in warmer, more acidic, and lower DO conditions (*28*, *29*). These changes in mean conditions may be especially important for species in the CCS, where these same three environmental drivers (i.e., temperature, pH, and DO) are negatively correlated with upwelling. Therefore, predicted changes in the mean due to climate change and OA (increases in temperature but decreases in pH and DO) will also alter their covariance. The covariance between temperature, pH, and DO is especially strong during upwelling season (*30*). Therefore, regions within the CCS that are more influenced by upwelling are also likely to experience greater deviations in the covariance structure of these three environmental drivers in response to global change compared to regions where environmental conditions are less influenced by upwelling.

We used a network of chemical sensors along the CCS to first characterize the natural covariance of temperature, pH, and DO in kelp forests from a region of intense upwelling (northern California) and a region of weak upwelling (southern California) (*21*, *24*). We then conducted a laboratory mesocosm experiment to assess the population-level differences in performance (i.e., survival, growth, calcification, metabolism, and grazing) of juvenile red sea urchins (*Mesocentrotus franciscanus*), consistent with local adaptation or acclimation across current mean pH, DO, and temperature conditions

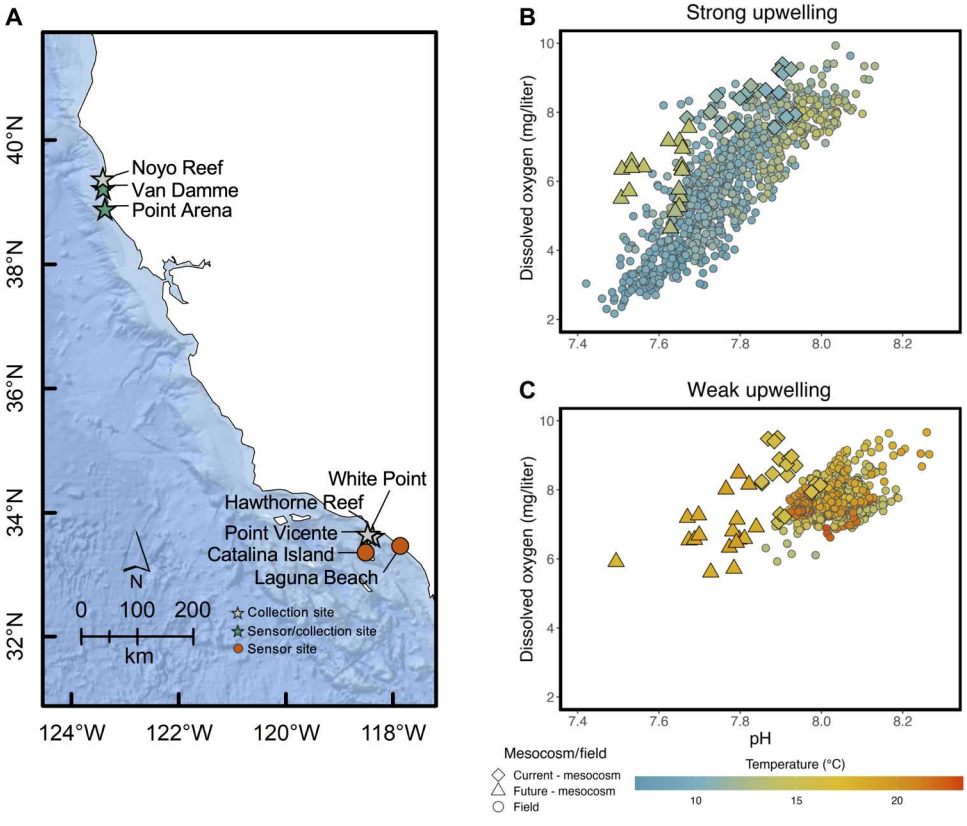

Fig. 1. Scatterplots of pH, oxygen, and temperature across study sites. Locations of sensor moorings and sea urchin collection sites along the coast of California are shown in (**A**). Diamond and triangle symbols indicate discrete sample measurements within experimental mesocosms for current and future treatments, respectively, while circles indicate daily mean conditions in the field. Scatterplot of time series data from oceanographic sensors deployed at a depth of ~15 m within kelp forests with daily mean experimental conditions as colored points. Data are from (**B**) two sites (Van Damme and Point Arena) exposed to strong upwelling and (**C**) two sites (Laguna Beach and Catalina Island) exposed to weak upwelling.

for each region in a common garden (i.e., both populations exposed to current treatments for both populations). *M. franciscanus* was used in this experiment because it is an economically important fisheries species (*31*) and an ecologically important grazer (*32*–*34*). *M. franciscanus* is found along the west coast of North America as far south as Baja, Mexico and as far north as Alaska and extending around the Pacific Ocean to Japan (*35*). Despite the potential for high gene flow via extended planktonic larval durations [62 to 131 days (*36*)] to limit local adaptation, work on *M. franciscanus* has shown genetic differentiation across populations due to both pre- and postsettlement selection (*35*). Within the same mesocosm experiment, we also tested for population divergence in response to region-specific projected future changes in pH, DO, and temperature, where the covariance between these factors is altered compared to the covariance associated with upwelling (i.e., each population was exposed to region-specific current and future treatments). If changes to covariance structure are more important than changes to mean conditions, then locally adapted/acclimated populations from intense upwelling regions may be more vulnerable to global change due to changes in the covariance structure. Temperature, pH, and DO are more tightly coupled in regions of intense upwelling than regions of weak upwelling, where temperature, pH, and DO have been less tightly coupled historically.

RESULTS

Regional differences in environmental regimes

Semicontinuous measurements of temperature, ocean pH, and DO between regions of strong (Point Arena and Van Damme) and weak (Catalina Island and Laguna Beach) upwelling in the CCS highlighted differences in mean conditions across sites (Fig. 1 and fig. S1). Specifically, Point Arena and Van Damme experienced lower mean pH, temperature, and DO conditions than Catalina Island and Laguna Beach (Table 1). We also reveal region-specific patterns of environmental covariance between strong and weak upwelling regions (Fig. 1, B and C). Although we found significant relationships between pH and DO, pH and temperature, and DO and temperature across all sites, the strength of these relationships differed between regions (table S1). At sites exposed to strong upwelling, pH and DO were tightly coupled, such that decreases in pH corresponded to decreases in DO [Point Arena: coefficient of determination (R^2) = 0.81; Van Damme: R^2 = 0.78]. Seawater pH and temperature, as well as DO and temperature, showed similar relationships in our strong upwelling region with low pH and DO corresponding to lower temperatures (Point Arena: pH versus Temperature, R^2 = 0.58; DO versus Temperature, R^2 = 0.55; Van Damme: pH versus Temperature, R^2 = 0.48; DO versus Temperature, R^2 = 0.37). Although statistically significant, these relationships were weaker at sites experiencing weaker upwelling (Catalina Island: pH versus DO, R^2 = 0.38; pH versus Temperature, R^2 = 0.04; DO versus Temperature, R^2 = 0.05; Laguna Beach: pH versus DO, R^2 = 0.05; pH versus Temperature, R^2 = 0.10; DO versus Temperature, R^2 = 0.06). This demonstrates that in regions experiencing strong upwelling, individuals are exposed to more predictable combinations of environmental conditions (i.e., a given pH only occurs for a narrow range of DO concentrations and temperatures).

Juvenile *M. franciscanus* from three replicate populations from these regions of intense upwelling versus relatively weaker upwelling were raised under current and projected future conditions for each region for 3 months. Current conditions were based on the mean temperature, pH, and DO conditions determined from sensor data, while future conditions were based on regional CCS climate projections for the year 2100 (*37*). Results of principal components analysis (PCA) analysis of in situ and experimental environmental data for the experiments highlight how the experimental treatment covariance aligned with the multivariate conditions currently experienced in the field. PC1 accounted for 92% of the variability and was primarily associated with mean daily temperature, while PC2 accounted for an additional ~8% of variation and is associated with mean daily pH and mean daily DO (Fig. 2). As expected, experimental conditions representing the current treatments within each region generally plot within the range of values experienced in the field (i.e., green and orange diamonds representing current experimental treatments overlap circles representing field conditions). Future conditions, however, generally do not overlap field conditions except for future experimental treatment conditions for the weak upwelling populations (i.e., green and orange triangles representing future treatment conditions generally do not overlap circles representing field conditions). Together, the correlations and PCA highlight how

Table 1. Environmental conditions across regions/treatments. Mean (± SD) daily in situ (field) environmental conditions from November 2017 to August 2021 within kelp forests from DuraFET (pH and temperature) and MiniDOT (DO) sensors. Mean (± SD) environmental conditions within the laboratory experiment (mesocosm). pH was measured from discrete water samples, and temperature and DO were measured with a YSI instrument.

Field/mesocosm	Site/treatment	Mean pH	Mean *T* (°C)	Mean DO (mg liter^{-1})
Field	Point Arena	7.78 ± 0.14	10.6 ± 1.55	5.82 ± 1.74
	Van Damme	7.72 ± 0.12	10.8 ± 0.92	6.22 ± 1.61
	Catalina Island	8.02 ± 0.05	17.3 ± 2.29	7.73 ± 0.45
	Laguna Beach	8.03 ± 0.06	15.7 ± 1.29	7.60 ± 0.33
Mesocosm	Strong upwelling current	7.84 ± 0.07	10.96 ± 0.17	8.41 ± 0.22
	Strong upwelling future	7.61 ± 0.06	13.44 ± 0.15	6.18 ± 0.31
	Weak upwelling current	7.91 ± 0.04	15.95 ± 0.08	8.43 ± 0.31
	Weak upwelling future	7.75 ± 0.03	18.59 ± 0.17	6.83 ± 0.28

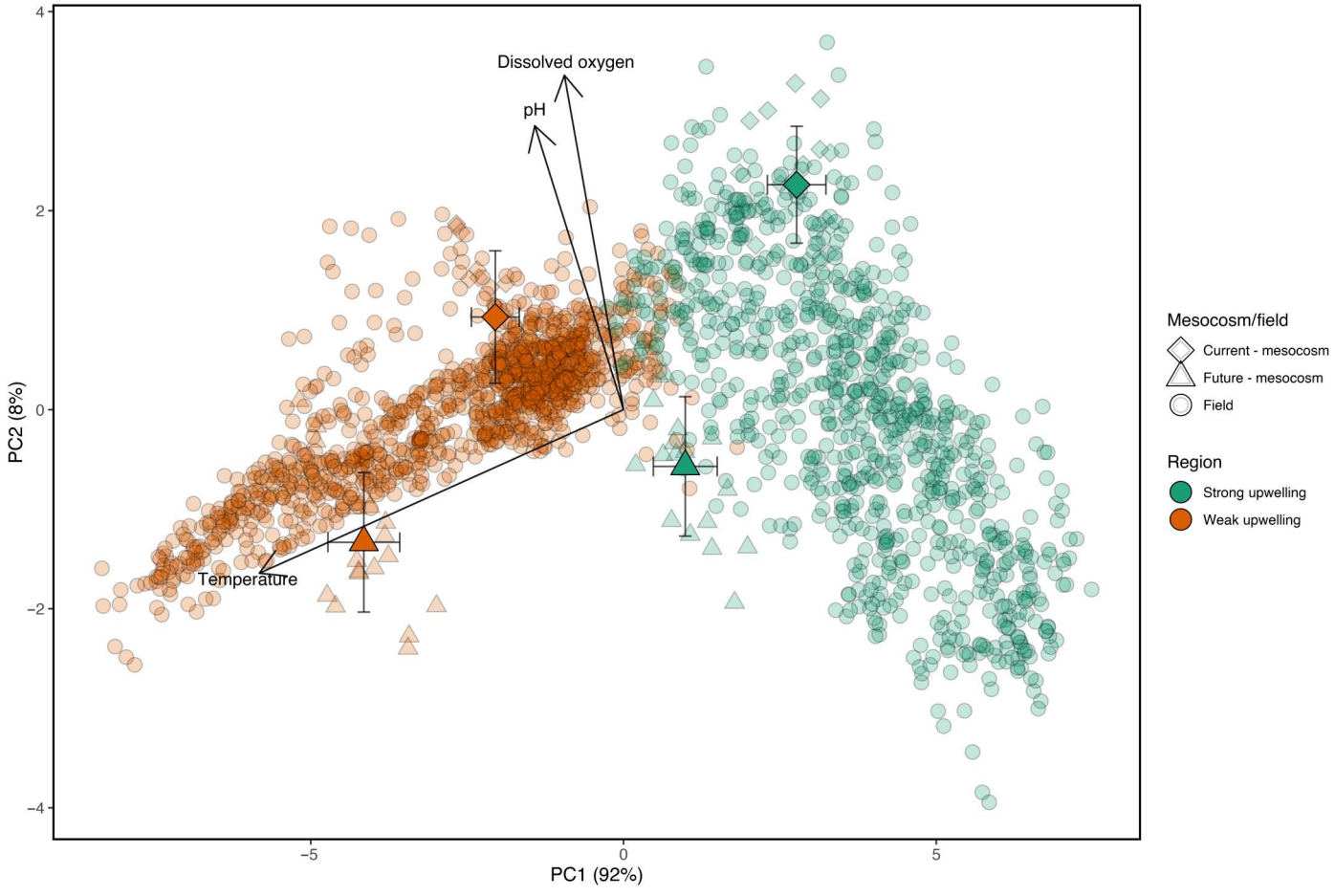

Fig. 2. PCA plot of in situ environmental (field) and laboratory (mesocosm) experimental conditions. Green symbols represent strong upwelling (cooler temperature) conditions, while orange symbols indicate weak upwelling (warmer temperature) conditions. Diamond and triangle symbols indicate discrete sample measurements within experimental mesocosms for current and future treatments, respectively, while circles indicate daily mean conditions (pH, DO, and temperature) in the field. Large symbols with error bars indicate the means ± SEM of PC scores for current and future experimental treatments for each region.

individuals within our strong upwelling region experience a much narrower range of temperatures for a given pH and DO combination, such that the projected warming creates conditions unlikely to occur in this region at present. This demonstrates how future changes, due to global change and OA, will have differential impacts on the covariance of pH, temperature, and DO across regions, leading to greater deviations from current conditions in strong versus weak upwelling regions.

Evidence for local adaptation/acclimation

After 3 months in common garden treatments (representative of current conditions in each region), sea urchins had significantly lower mortality in their respective home environments, consistent with local adaptation/acclimation (Fig. 2A and table S2). In particular, mortality increased among the populations from weak upwelling when raised under strong upwelling conditions compared to the populations from strong upwelling conditions (Fig. 3A and table S3). We also find increased mortality among the populations from strong upwelling when raised under weak upwelling conditions compared to the populations from weak upwelling conditions (Fig. 3A and table S3).

Growth and net calcification also differed across treatments and populations, consistent with local adaptation and acclimation (table S2). Although sea urchins from weak upwelling conditions have higher growth and net calcification under current conditions overall (Fig. 3, B and C, and table S3), the slope of the reaction norms for growth differed between populations (i.e., there was a significant population x treatment interaction; table S2). Growth in sea urchins originating from our weak upwelling region was 350% higher than that in sea urchins from our strong upwelling region under weak upwelling conditions compared to only 34% higher under strong upwelling conditions.

We found that metabolic rates (energetic costs) were elevated in individuals from strong upwelling conditions compared to those from weak upwelling conditions (Fig. 3D and table S2). Body condition (gonad–to–somatic tissue ratio) was also greater in sea urchins from the sites exposed to strong upwelling, both initially and after 3 months in experimental treatments (fig. S2, A and B, and table S2). In contrast, energetic gains (measured via consumption) for both populations were greater under weak upwelling conditions than strong upwelling conditions (Fig. 3E and table S2).

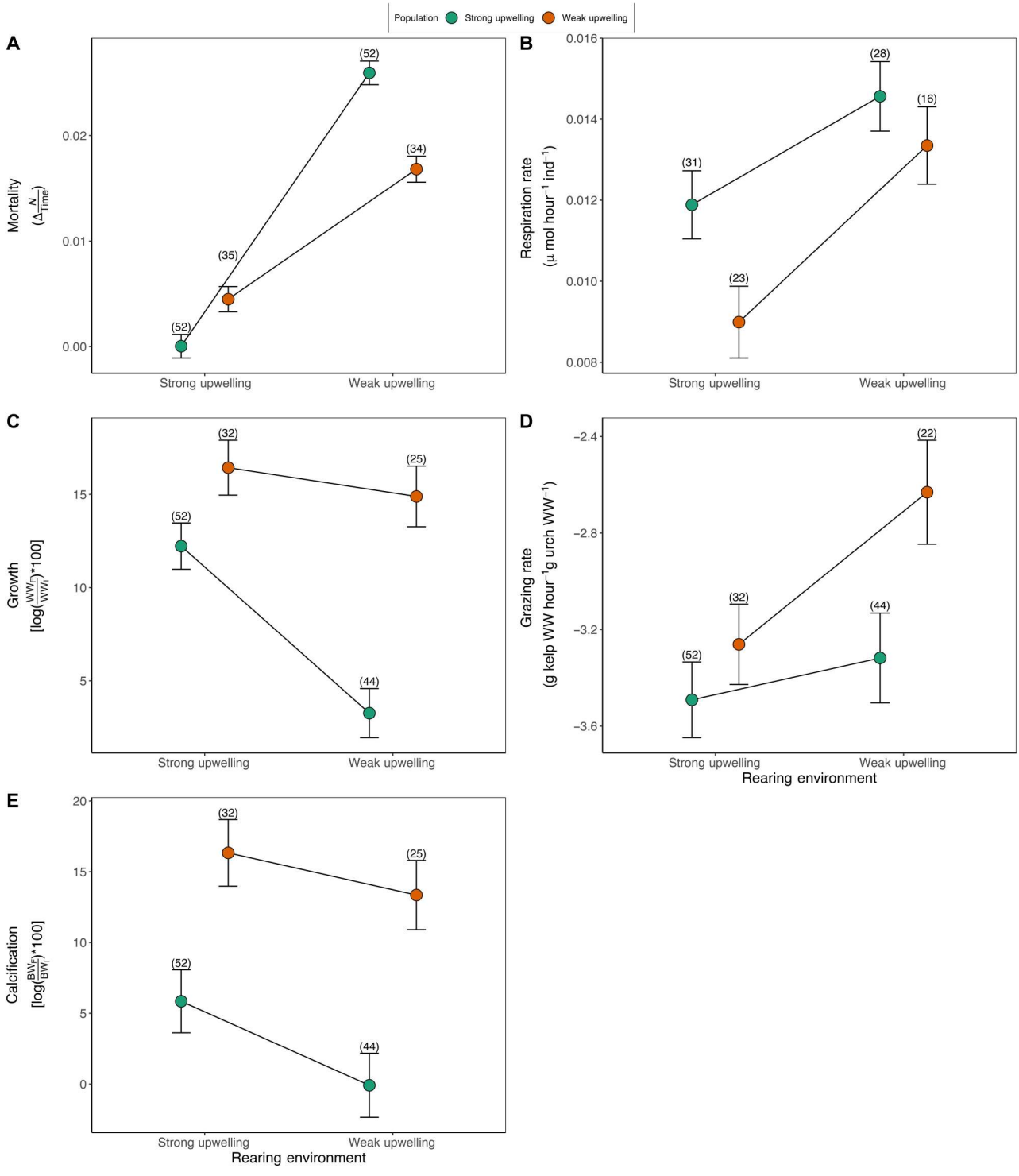

Fig. 3. Species performance in common garden experiment. Performance metrics across sea urchin populations reared for 3 months with (**A**) mortality, (**B**) respiration rate, (**C**) growth, (**D**) grazing rate, and (**E**) calcification of sea urchins from strong upwelling and weak upwelling regions reared under current conditions for both strong and weak upwelling regions. Points represent the mean, and error bars indicate the SE. Numbers above bars indicate replicates, and lines connecting populations indicate reaction norms.

Looking to the future

Populations of sea urchins from weak upwelling regions were more vulnerable to future environmental conditions than sea urchins from strong upwelling regions. After 3 months in the current and projected future treatments for each region, mortality increased in future treatments for both populations (Fig. 4A and tables S4 and S5). Mortality increased from 0.0001 to 0.0125 N day^{-1} from current to projected future conditions in the populations from strong upwelling and from 0.0135 to 0.0463 N day^{-1} from the current to projected future conditions in the populations from weak upwelling conditions.

Growth and net calcification were reduced under future ocean conditions for both populations, but there was no effect of population origin (Fig. 4, B and C, and table S4). We did not detect an effect of population or future ocean conditions on metabolic rates (table S5). However, grazing rates were elevated in individuals from our weak upwelling populations compared to our strong upwelling populations (Fig. 4D and table S5). Furthermore, we found that strong upwelling populations had better body condition, with higher gonad–to–somatic tissue ratios than the weak upwelling populations, which could underlie population differences in mortality (fig. S2C and table S4).

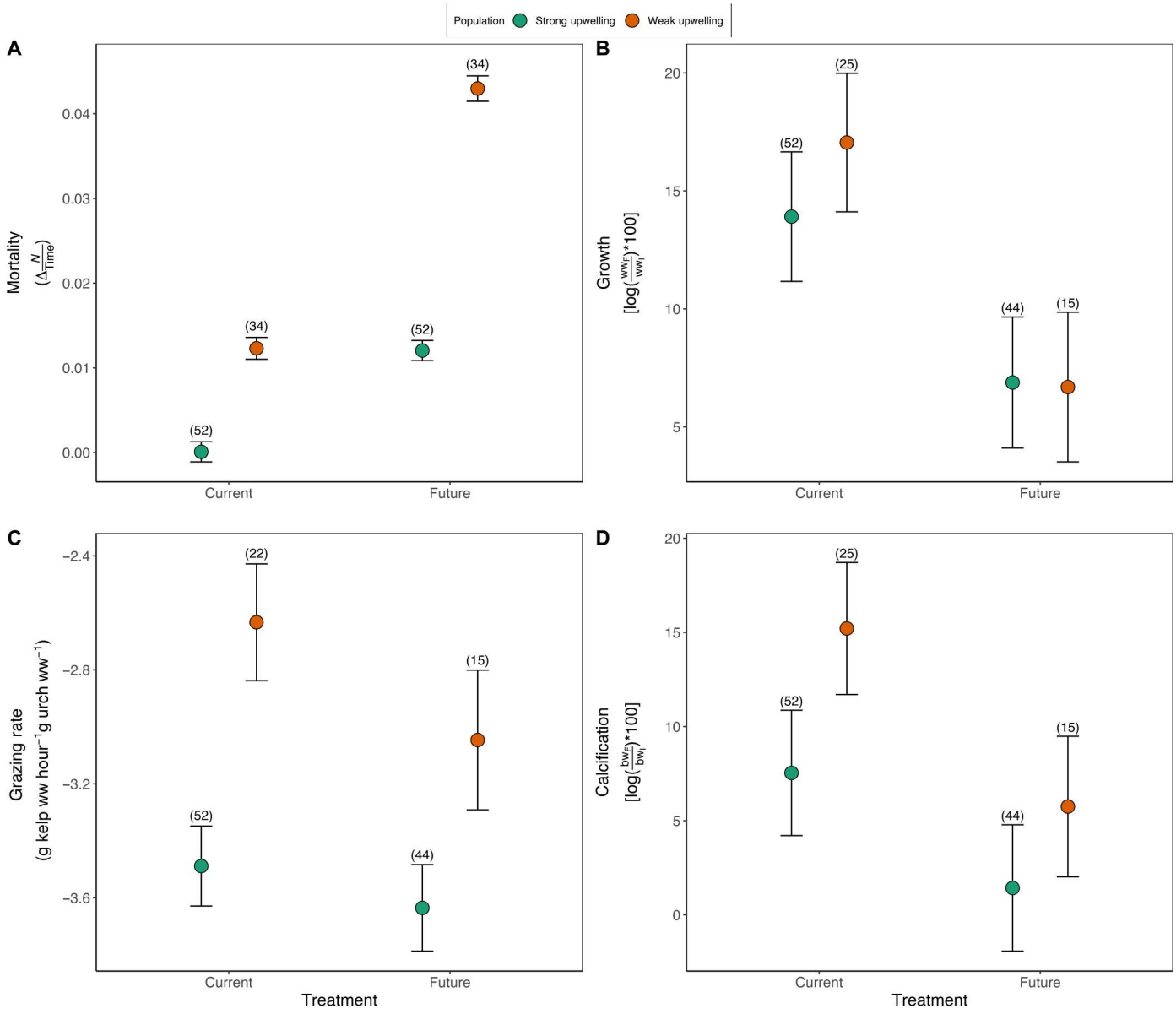

Fig. 4. Species performance in climate change experiment. Performance metrics across sea urchin populations reared for 3 months with (**A**) mortality, (**B**) growth, (**C**) grazing rate, and (**D**) calcification of sea urchins from strong upwelling and weak upwelling regions reared under region-specific current and future conditions. Points represent the mean, and error bars indicate the SE. Numbers above bars indicate replicates.

DISCUSSION

Understanding the capacity for organisms to adapt to environmental change is central to global change biology. Most studies on local adaptation and acclimation to environmental change have focused on one driver (e.g., temperature and pH); thus, little is known about the potential for evolutionary rescue to multiple, concurrent changes in the environment. Here, we found evidence for local adaptation/acclimation to multivariate environmental regimes across populations of red sea urchins, *M. franciscanus*, found along the coast of California. Although it is possible that our results show true adaptive responses because of the removal of field acclimation or other nongenetic effects (e.g., maternal effects) during our 3-month holding period, we cannot, with certainty, attribute the results of our common garden experiment to local adaptation (i.e., genetic differences). These locally adapted/acclimated populations did, however, differ in their susceptibility to future environmental changes in multiple environmental drivers, with sea urchins from a weaker upwelling region showing greater sensitivity to the negative impacts of climate change and OA. This work supports more recent efforts to improve ecological models predicting the effects of climate change and OA on marine species and ecosystems by incorporating intraspecific variation (*8*, *38*).

For the red sea urchin, *M. franciscanus*, we show evidence consistent with local adaptation/acclimation to complex, multivariate environmental regimes. However, although both populations performed better in their home regimes, mortality (in sea urchins originating from both regions) was higher under current weak upwelling conditions compared to current strong upwelling conditions (Fig. 3A and table S3). Although we are not able to tease apart the effects of any single environmental driver on these results, given that we manipulated temperature, pH, and DO in combination to reflect their covariance in nature, it is likely that thermal stress contributed to the higher overall mortality under the current weak upwelling conditions. This interpretation is based on DO concentrations being similar between the two current treatments and pH being higher in the current weak upwelling treatment (i.e., higher pH should be less stressful; Table 1). Therefore, sea urchins from weaker upwelling conditions may have higher survivorship under these conditions because of a higher thermal tolerance to cope with the naturally warmer seawater temperatures associated with the region. It is unclear, however, whether there is a cost to increased thermal tolerance in the sea urchins adapted/acclimated to warmer, weak upwelling conditions.

We also found that growth and net calcification were higher, overall, in sea urchins from our weak upwelling region under both current treatment conditions (Fig. 3, C and E, and table S3). These results are consistent with the work by Pespeni *et al.* (*39*) that found higher scope for growth and calcification in purple sea urchins, *Strongylocentrotus purpuratus*, from San Diego, CA than from Boiler Bay, OR when reared in a 3-year-long common garden experiment. These differences in scope for growth and calcification corresponded with higher expression of genes related to biomineralization in the population from San Diego, CA. It is possible that underlying differences in gene expression between our populations could also play a role in the higher growth and calcification in sea urchins from our weak upwelling region. The slopes of the reaction norms across treatment conditions differed between populations, with a steeper slope for sea urchins from the strong upwelling region than the weak upwelling region. This suggests that although sea urchins from our weak upwelling region outperformed sea urchins from our strong upwelling region in both current treatments within our mesocosm experiment, it is likely that sea urchins from our strong upwelling region will have a higher performance than sea urchins from our weak upwelling region when exposed to higher-intensity upwelling conditions (which do occur naturally in our strong upwelling region). Future work to better understand how performance shifts across a range of environmental conditions at each location will be an important next step to understand the potential of success for techniques such as assisted migration.

Body condition (gonad–to–somatic tissue ratio) was higher in sea urchins from the strong upwelling region (fig. S2). Energetic costs (measured by metabolic rates) were also greater in sea urchins from strong upwelling regions, perhaps because of the increased energetic demands of maintaining reproductive tissue (table S2). Together with our findings for growth and calcification, these results suggest that sea urchins from the different populations may have been allocating energy differently (i.e., prioritizing overall growth and net calcification versus gonad production). This hypothesized difference in energy allocation could be due to differences in phenology, the duration of time spent in a starved state (i.e., differences in timing/duration of urchin barren formation across regions), or ecological factors unrelated to the environmental conditions. For example, differences in the phenology of gametogenesis, which occurs over multiple seasons in sea urchins, could explain differences in gonad production between sites. The timing of egg production and development has been shown to differ across latitudes for other marine species because of differences in temperature regimes (*40*). Seasonality can also lead to differences in energy partitioning between growth and reproduction, if attaining a larger size leads to higher overwintering survivorship (*41*). Alternatively, trade-offs between growth and other processes could explain the differences seen here across populations (*42*, *43*). For instance, higher predation rates can select for rapid growth to larger sizes in fishes (*44*).

In addition, although all sea urchins in our study were collected from barrens, differences in the duration and extent of barren history across populations could have contributed to differences in the initial condition of sea urchins [e.g., barren conditions from regions of weak upwelling are much older (*45*) and more persistent than those in regions of strong upwelling (*46*)]. To account for these differences, sea urchins were reared in the laboratory for 3 months and fed weekly. Past studies have shown that gonads of the purple sea urchin, *S. purpuratus*, can recover from starvation after 2 to 3 months (*32*). After 3 months of ad libitum feeding and before the start of our experiment, we still found significantly lower body condition in sea urchins from sites in our weak upwelling region. Regardless of the environmental conditions, sea urchins from the weak upwelling sites not only maintained lower body condition throughout the common garden experiment (fig. S2B) but also demonstrated higher growth and net calcification rates (Fig. 3, C and E). Future work assessing the role that environmental and ecological factors (e.g., barren history, phenology, and predation) play in shaping energy allocation across populations of sea urchins will be important to understand the mechanistic underpinnings of differences in species′ responses to environmental change.

Despite strong evidence for local adaptation/acclimation of the populations to their respective environmental regimes, we did find differences in susceptibility to region-specific projected future change despite the changes in environmental conditions being similar in magnitude across regions. Specifically, sea urchins from the warmer, weaker upwelling conditions were more vulnerable to projected future changes. These findings contrast with our hypotheses that populations from intense upwelling conditions would be more vulnerable to future change because of the tight coupling of environmental drivers in these regions and subsequent alterations to the covariance structure with future change. Because the absolute values of the environmental conditions differed among future treatments for each population, we cannot completely disentangle the effects of changes in covariance from the treatment values. However, higher vulnerability of the locally adapted/acclimated population from warmer, weaker upwelling suggests that thresholds in tolerance to single drivers (i.e., temperature) or deviations from current conditions may be as or more important than changes in covariance over the range of conditions used here. This is based on the populations from weaker upwelling experiencing the warmest temperatures of any treatment in their future scenario. This interpretation is consistent with previous findings (*16*) that biotic responses can be driven by a single dominant environmental driver. Alternatively, the higher vulnerability of the populations from weaker upwelling regions to future change could be due to the changes in pH and DO deviating from the relatively narrower range of conditions experienced in the field (Fig. 1). Last, the temporal scale of variability, and, potentially, the predictability, in environmental conditions also differed between the regions (fig. S1), and this variability could play an important role in shaping species′ responses to change (*3*). For example, variable environments could select for plasticity (*47*) with implications for adaptation (*48*). Future work assessing how different temporal scales of environmental variability (i.e., diel, semidiel, and seasonal) or predictability alter species′ performance will help to further elucidate the role of variability in structuring evolutionary responses to global change.

Our results indicating higher vulnerability of the warm-adapted/acclimated populations from regions of weak upwelling are also in line with past work on range shifts and thermal physiology, which suggest that additional warming within warm regions of a species range has the potential to push species beyond thermal tolerance limits, leading to localized extinction (*49*, *50*). However, our short-term (83-day) laboratory experiment does not capture many important aspects of global change that occur over time. For example, recent work by Coleman *et al.* (*51*) found that mass mortality of the kelp *Ecklonia* due to a marine heat wave led to "genetic tropicalization," whereby surviving individuals and new recruits had a shift in alleles from cool water types to warm water types. Similarly, Brennan *et al.* (*4*) demonstrate shifts in allele frequencies due to differential survival of larval purple sea urchins, *S. purpuratus*, exposed to extreme pH. These studies suggest that exposure to extreme environmental conditions associated with global change can lead to rapid evolution of more tolerant phenotypes, which may be beneficial as changes in the mean occur more slowly. We were, however, unable to measure the underlying genetic changes due to differential mortality in our study. Although our work suggests higher vulnerability to future change for the populations near the warm edge of the range for *M. franciscanus*, it is unclear whether red sea urchins will experience a range contraction due to environmental change or adapt to changing conditions via genetic tropicalization from warm-adapted phenotypes. Future work focused on understanding shifts in underlying allele frequencies could provide important insights into the potential of evolutionary rescue of southern populations at risk to future climate change.

Climate change and OA have been shown to reduce growth and calcification across a wide range of species (*52*). Here, we find reductions in growth and calcification under future conditions for both populations (Fig. 4, B and D, and table S4). Growth and calcification rates were similar across populations in respective current and future environmental regimes. Although it is still unclear why body condition was higher at the outset of the experiment in sea urchins from strong upwelling populations, the maintenance of reproductive tissue while maintaining growth and calcification rates similar to those of sea urchins from weak upwelling conditions suggests that energetic costs may be elevated for sea urchins from weak upwelling conditions. Furthermore, sea urchins from weak upwelling regions also had elevated grazing rates (i.e., higher energetic gains), suggesting that they were unable to fully compensate for any increased energetic costs. We did not detect differences in metabolic rates between populations and treatments in our climate change experiment. This suggests that future environmental changes are unlikely to result in rising maintenance costs, although it may affect other aspects of an organism′s energy budget not measured here. Future work that uses a bioenergetic approach is crucial to further understanding how differences in energy allocation across sea urchin populations contribute to the differences in susceptibility to future climate changes seen here.

For the duration of our experiments, urchins were fed biweekly to ensure sufficient growth. Access to food, however, is a key issue for sea urchins inhabiting urchin barrens, with many urchins living at starved states for extended periods of time. Therefore, results shown here may underestimate the true impacts of global change on sea urchins inhabiting urchin barrens, if energetic gains via consumption help to compensate for the detrimental effects of climate change and OA. Projected increases in the frequency and duration of extreme climatic events (i.e., marine heat waves) due to global change are likely to increase the formation of urchin barrens worldwide. To better understand the true consequences of global change on sea urchin populations, future work should assess the impacts of climate change and OA on sea urchins across multiple levels of food availability likely to occur in nature.

Together, our results highlight that using a species′ response to global change from one population to predict another populations′ response may not be appropriate (*40*). Local adaptation/acclimation can alter how species respond to multivariate environmental change; however, we hypothesize that thresholds in tolerance for single environmental drivers may be more important than changes in the covariance structure of their environmental regime for survival. Across populations, differences in energetic costs and energy allocation strategies likely play an important role in how species respond to future environmental change. Future work linking the molecular and bioenergetic underpinnings of differences in species′ responses to multivariate environmental change across populations is crucial to gaining a more mechanistic understanding of how and why species abundances and distributions might shift in the future.

MATERIALS AND METHODS

Experimental design

Environmental monitoring

To determine the mean and covariance in environmental conditions that organisms currently experience within kelp forests along the coast of California, we established an array of monitoring locations for the deployment of autonomous pH, temperature, and DO sensors. We chose two sites in northern California (Point Arena, 38.9460°N, 123.7389°W; Van Damme, 39.2711°N, 123.7948°W) and southern California (Laguna Beach, 33.5421°N, 121.9459°W; Catalina Island, 33.4412°N, 118.4654°W; Fig. 1A). Our northern California sites experience stronger upwelling and will be referred to as "strong upwelling" sites, whereas our southern California sites experience weaker upwelling and will be referred to as "weak upwelling" sites. We collected data continuously (every 10 min) from around November 2017 to August 2021, with the exception of some gaps in measurements due to sensor malfunctioning that typically occurred during the first 2 years of data collection. Custom-built pH and temperature sensors containing the Honeywell Durafet pH sensors were used for this study (*53*). The pH sensors were calibrated by injecting the flow cell with equimolar tris in artificial seawater solution (*54*), a standard pH solution for seawater pH (*55*). Sensors were calibrated at the time of deployment and recovery, and the calibration from the deployment was preferentially used because of potential biofouling or sensor malfunctioning by the time of recovery. DO was measured using a MiniDOT, measuring every 10 min (Precision Measurement Engineering), co-located to the pH sensor. These sensors were calibrated in DO-saturated seawater before each deployment (*53*). All sensor data were resampled to calculate daily means before data analyses. We determined the relationships between daily mean pH and temperature, pH and DO, and temperature and DO at our sites using linear regression.

Collection sites

We identified three sites in our strong upwelling region and three sites in our weak upwelling region to collect red sea urchins, *M. franciscanus*, for our experiment examining (i) evidence for local adaptation to environmental regimes and (ii) testing the effects of future environmental change across populations. We collected *M. franciscanus* individuals [test diameter = 3.7 ± 1.1 cm (means ± SD)] using SCUBA (~10 m of water depth) from strong upwelling sites at Point Arena, CA (38.9460°N, 123.7389°W) on 7 October 2020; Van Damme, CA (39.2711°N, 123.7948°W) on 19 October 2020; and Noyo Reef, CA (39.4283°N, 123.8107°W) on 5 November 2020 and from weak upwelling sites at White Point, CA (33.7125°N, 118.3185°W); Point Vicente, CA (33.7400°N, 118.4140°W); and Hawthorne Reef, CA (33.7470°N, 118.4159°W) on 18 November 2020. We chose strong upwelling collection sites because of their proximity to two oceanographic monitoring sites (Point Arena, CA and Van Damme, CA) with which we have long-term data to characterize pH, temperature, and DO conditions. Because red sea urchins are not as common in southern CA, we chose our weak upwelling collection sites based on local knowledge of red sea urchin abundances and proximity to existing HOBO (Onset) temperature logger data, which we were able to use to confirm similarities in temperature between monitoring and collection sites (fig. S3). After collection, we placed sea urchins in a dry cooler sandwiched between kelp and immediately transported them to Long Marine Laboratory (LML) at the University of California, Santa Cruz. Upon arrival at LML, we immediately placed urchins from different sites into separate water tables and supplied them with flow-through seawater from just offshore of the marine laboratory. Although we were unable to continuously measure environmental conditions within the holding tanks, mean daily temperature (± SD) of incoming seawater at the marine laboratory during the holding period was 12.09° ± 1.48°C. We fed sea urchins fresh giant kelp, *Macrocystis pyrifera*, once a week until the start of the experiment (~3 months).

Mesocosm system

The mesocosm system at LML is supplied with ambient ultraviolet (UV)–filtered seawater. This seawater flows into two large (500-gallon) sumps: a "hot" sump that warms incoming ambient seawater to ~24°C via three 9000-W heaters (Optima Plus Compact Aquatic Heater, Aqua Logic Inc.), and a "cold" sump that is chilled to ~8°C by a water-cooled chiller (Multi Temp Water-Cooled Marine Duty Chiller, Aqua Logic Inc.; fig. S4). We plumbed seawater from both sumps to a temperature blending valve system (TBS; Aqua Logic Inc.) where we blended hot and cold seawater to create four static temperature conditions representing current and future conditions in both northern and southern CA. Each temperature treatment fed three replicate 5-gallon "header" buckets fit with a gamma lock seal containing a Durafet pH probe and DO sensor (GoDirect Optical Dissolved Oxygen, Vernier). Each header tank supplied flow-through seawater to two replicate "bins" that housed the sea urchins in our study. To manipulate the pH and DO of our treatment water, a third "upwelled seawater" sump was used to create cold, acidic, and low-DO seawater. This sump was supplied with cold seawater from the same cold seawater sump used to supply the blending valves. Pure CO_2 was continuously bubbled into the upwelled seawater sump until it reached a desired set point of pH 7.3. The pH of this tank was controlled with a feedback loop using a Durafet pH sensor and a custom LabVIEW program that actuated a mass flow controller (SmartTrak 50, Sierra Instruments) to allow the flow of CO_2 into the sump. DO of the "upwelled" sump was manipulated by continuously bubbling pure N_2 gas at a rate of ~10 liters min^{-1}. N_2 gas was supplied via a nitrogen generator (MNG-1010, Compressed Gas Technologies Inc.). Although we did not control or monitor the DO concentrations in the acidic/low-DO sump, preliminary testing suggested that the DO concentration was ~4.0 mg $liter^{-1}$.

All 12 header buckets (3 buckets at each of the four temperature levels) were supplied with mixed seawater from the TBS with small amounts of acidic/low-DO seawater using a feedback system. Briefly, the feedback system triggered solenoids to open and allow acidic/low-DO seawater in whenever pH drifted above a desired set point. Because pH and DO are coupled in this system, our pH control created four distinct temperature, pH, and DO treatments mimicking current and future projected conditions at each location (strong upwelling current, pH 7.8, DO = 8.0 mg $liter^{-1}$, and temperature = 10°C; strong upwelling future, pH 7.6, DO = 6.0 mg $liter^{-1}$, and temperature = 13°C; weak upwelling current, pH 8.0, DO = 8.0 mg $liter^{-1}$, and temperature = 16°C; weak upwelling future, pH 7.8, DO = 6.0 mg $liter^{-1}$, and temperature = 19°C). These temperature and pH treatments represent the mean temperatures measured within the kelp forest at each region during our monitoring period and a +3°C, −0.2 pH unit future treatment based on projected regional warming and acidification by the end

of the year 2100 (*29*, *37*). Because of logistical difficulties scrubbing oxygen from our system, DO concentrations are slightly higher than that of current and future conditions for both regions but represent conditions currently experienced by organisms within each location and are consistent in direction with expectations (i.e., future conditions are ~2 mg liter^{-1} lower than current). Each of the 12 header buckets had two outflows that connected to replicate ~20-gallon experimental bins that housed 12 to 15 individually caged sea urchins (N = 1 to 2 for each site from the weak upwelling region and N = 2 to 3 for each site from the strong upwelling region; fig. S4) with a flow rate of ~20 gallons hour^{-1}. Between ~10:00 a.m. and 2:00 p.m. every day, we measured the pH, temperature, DO, and salinity in each bin using a multimeter (YSI Quatro, Yellow Springs Instruments Inc.). We collected discrete samples for total alkalinity (TA) and spectrophotometric pH from each header bucket and bin containing sea urchins every 2 to 3 weeks for the duration of the experiment (N = 6 time points). Using best practices (*56*), we made spectrophotometric pH measurements using *m*-cresol purple (Shimadzu UV-1800, Shimadzu) and TA measurements using open-cell titration (905 Titrando, Metrohm). Instruments were validated using certified reference materials from the laboratory of A. Dickson (Scripps Institution of Oceanography) at the beginning and end of each day that the samples were processed. We used TA and spectrophotometric pH measurements from discrete samples, salinity, and temperature from YSI measurements and stoichiometric dissociation constants defined by Mehrbach *et al.* (*57*) and refit by Dickson and Millero (*58*) to calculate the entire carbonate system across treatments and to calibrate Durafet electrodes within header buckets (fig. S5 and table S6).

To assess the potential of adaptation/acclimation to local environmental regimes and understand the effects of future environmental change on sea urchins, we reared *M. franciscanus* individuals in a common garden climate change experiment exposing individuals to current and future regimes for 83 days (13 February to 15 May 2021). Within each replicate experimental bin, sea urchins were placed in individual 0.5-liter cages where they were fed ~1 g of kelp twice a week for the duration of the experiment. If kelp was present in the cage at the time of feeding, which was usually the case, then it was replaced by fresh kelp.

Mortality

We recorded the deaths of sea urchins across treatments and populations for the duration of the experiment. We opened all cages daily and visually assessed each individual urchin for death or disease. If an urchin died, we immediately removed it from the experiment, and any signs of disease were noted. For each day of the experiment, we calculated the number of surviving urchins.

Growth and net calcification

Before being placed into their respective experimental treatments and after 83 days under treatment conditions, we measured wet-weights and buoyant-weights of each urchin to calculate a relative growth and net calcification rate. Because of the large number of urchins in the experiment, we measured all individuals from just one site at a time and placed them in the system on the same day. Therefore, the experiment's start days and end days were staggered across sites over approximately 1 week, and no anomalies in environmental conditions occurred during these time periods that may confound the results.

We measured wet weights by first carefully patting each sea urchin with a paper towel to remove large water droplets. We then placed sea urchins on a scale and measured their weight to the nearest 0.001 g. To obtain buoyant weights, a proxy for calcified biomass (*59*), we placed sea urchins in a basket connected by monofilament to the bottom of a weigh-below balance. The basket (with sea urchin) was fully submerged in seawater and measured to the nearest 0.001 g. We calculated the relative growth rate (RGR) as

$$\mathrm{RGR} = \left[\mathrm{Log}\left(\frac{\mathrm{WW_F}}{\mathrm{WW_I}}\right)\right] * 100$$

where $\mathrm{WW_I}$ and $\mathrm{WW_F}$ are the initial and final (after 83 days) wet weights, respectively. We calculated relative net calcification rate (RCR) as

$$\mathrm{RCR} = \left[\mathrm{Log}\left(\frac{\mathrm{BW_F}}{\mathrm{BW_I}}\right)\right] * 100$$

where $\mathrm{BW_I}$ and $\mathrm{BW_F}$ are the initial and final (after 83 days) buoyant weights, respectively. In total, 11 urchins were excluded from growth analyses because of outward signs of disease, which were not associated with any particular treatment or experimental bin.

Gonad–to–somatic tissue ratio

Because gonad production can be a proxy for body condition in sea urchins, we were interested in assessing the impacts of environmental conditions on the gonadal–to–somatic tissue ratios. At the beginning and end of the experiment, we dissected sea urchins to separate gonad tissue from the remaining somatic tissue using forceps. At the beginning of the experiment, we euthanized individuals from each site to understand differences at the outset of our experiment. Gonad and somatic tissues were placed into foil packets and dried in the drying oven at 80°C for 24 hours. Foil packets with dried tissue were weighed to 0.001 g before being placed in a muffle furnace at 550°C for 8 hours to obtain ash-free dry weights (AFDWs). Following combustion, foil packets were reweighed, tissue weight (gonad or somatic) was calculated as the change in weight before and after combustion (AFDW), and the gonad–to–somatic tissue ratio (G:S) was calculated as

$$G{:}S = \frac{G_{\mathrm{AFDW}}}{S_{\mathrm{AFDW}}}$$

where G_{AFDW} is the AFDW of gonad tissue and S_{AFDW} is the AFDW of somatic tissue.

Grazing and metabolism

After 83 days of exposure to our treatment conditions, we measured the grazing and metabolic rates of sea urchins to assess whether future environmental conditions alter the balance between energetic costs (metabolism) and energetic gains (grazing) and to assess the potential of local adaptation/acclimation to regional environmental conditions. Forty-eight hours before grazing assays, we removed kelp from sea urchin cages and starved individuals to reduce the potential effects of digestive status on metabolism measurements. To measure the standard metabolic rates of individuals, we followed methods outlined by Donham *et al.* (*30*). Briefly, we placed individual sea urchins into polycarbonate respirometry chambers (either ~100 or ~230 ml, depending on the size of the urchin) with seawater from their respective treatment. In addition, we used control chambers (without urchins) to measure the effects of water column processes on changes in DO over time. We sealed chambers from the external environment and used a stir bar within each chamber to

continuously mix seawater and a DO sensor spot (PSt3, PreSens Precision Sensing GmbH) to measure DO within the chamber using a fiber optic oxygen reader (Fibox 4, PreSens Precision Sensing GmbH). We placed sealed chambers on a multiposition magnetic stirring system (2mag MIXdrive) submerged in a water bath, maintaining the respective treatment conditions with 3 to 8 sea urchins (in weak upwelling urchin assays) or 6 to 15 sea urchins (in strong upwelling urchin assays) and three control incubations to run simultaneously. Because of the size of the magnetic stirring system, we were unable to assay more than 15 sea urchins per run and only a single run per site. Differences in sample sizes were due to differences in initial samples sizes between regions/sites and differential mortality across treatments. We measured DO concentrations seven times over a ~30-min incubation and used local linear regression to fit measurements of DO as a function of time using LoLinR in R (*60*). All incubations were approximately linear over the duration of the incubations and were not allowed to fall below 3.75 mg liter^{-1}. We corrected the slopes (metabolic rate) of each sea urchin with an average of the slopes of controls that were run in the same run. Standard metabolic rate was mass-corrected using the mean mass of all individuals and mass correction equations from Steffensen *et al.* (*61*).

Following metabolic assays, we returned sea urchins to their cages within their respective treatments and presented individual urchins a single preweighed disc of kelp (~7 cm in diameter). After 24 hours, we removed and reweighed the remaining kelp disc. We calculated the mass-corrected grazing rate as the change in wet weight of kelp after 24 hours, divided by the mass of the individual sea urchin. In total, 11 urchins were excluded from the final grazing assay because of outward signs of disease. Three additional urchins escaped their cages during the grazing assay, and we were unable to calculate a grazing rate for these individuals.

Statistical analysis

We ran two sets of models for each response variable to assess (i) the potential of local adaptation to environmental regimes across *M. franciscanus* populations and (ii) the differences in the impacts of future environmental change across populations. We fit the number of deaths to linear mixed models with time, treatment, population, and mean weight (calculated from the initial weight at each time step) as fixed effects and site nested in population as random effects using lmer in R. Mean initial weight was used to control for any effect of size-dependent mortality. If a significant three-way interaction was found, then contrasts were conducted on slopes of regressions calculated using emtrends in R to test whether (i) mortality under current local conditions differs from the distant populations′ mortality in the current local treatment (i.e., strong upwelling populations under current strong upwelling conditions versus weak upwelling populations under current strong upwelling conditions; weak upwelling populations under current weak upwelling conditions versus strong upwelling populations under current weak upwelling conditions) and (ii) mortality under current local conditions differs from that under future local conditions (i.e., strong upwelling populations under current strong upwelling conditions versus strong upwelling populations under future strong upwelling conditions; weak upwelling populations under current weak upwelling conditions versus weak upwelling populations under future weak upwelling conditions).

We fit relative growth and net calcification rates to linear mixed models with population, treatment, and weight as fixed effects and header nested in treatment, site nested in population, and bin nested in header, which was nested in treatment, as random effects. We log-transformed the covariate of weight to linearize the relationship between relative growth and net calcification rates and weight. If significant effects of population and treatment were found, then contrasts were conducted on estimated marginal means calculated using emmeans in R.

We fit the initial gonad–to–somatic tissue ratio to linear mixed models with population and weight as fixed effects and site nested within population as random effects. Last, we fit the final gonad–to–somatic tissue ratio to linear mixed models with population, treatment, and weight as fixed effects and header nested in treatment, site nested in population, and bin nested in header nested in treatment as random effects. Because weight was a covariate in these models, we removed nonsignificant interactions with weight and reran statistical models.

We fit grazing and metabolic rate to linear mixed models with the same fixed and random factors for growth and calcification, excluding the fixed effect of weight, which was accounted for by mass correction of grazing and metabolic rates. Grazing rates less than 0 were transformed to zero because negative grazing rates are not possible and were due to error in wet weight measurements. We log-transformed grazing rate to meet assumptions of normality. Because zeros were present in our nontransformed grazing data, we first transformed grazing rates using the equation

$$G_t = \mathrm{Log}(G_r + C)$$

where G_r is the nontransformed grazing rate, G_t is the transformed grazing rate, and C is a constant added so that grazing rates are greater than 0. We chose a value of C equal to 10% of the mean to have little effect on G_r because values of G_r ranged between 0 and 1. All models were fit using lmer in R.

Supplementary Materials

This PDF file includes:

Figs. S1 to S5
Tables S1 to S6

REFERENCES AND NOTES

1. M. L. DeMarche, D. F. Doak, W. F. Morris, Incorporating local adaptation into forecasts of species' distribution and abundance under climate change. *Glob. Change Biol.* **25**, 775–793 (2019).
2. J. M. Barley, B. S. Cheng, M. Sasaki, S. Gignoux-Wolfsohn, C. G. Hays, A. B. Putnam, S. Sheth, A. R. Villeneuve, M. Kelly, Limited plasticity in thermally tolerant ectotherm populations: Evidence for a trade-off. *Proc. Biol. Sci.* **288**, 20210765 (2021).
3. M. C. Bitter, L. Kapsenberg, K. Silliman, J.-P. Gattuso, C. A. Pfister, Magnitude and predictability of pH fluctuations shape plastic responses to ocean acidification. *Am. Nat.* **197**, 486–501 (2021).
4. R. S. Brennan, A. D. Garrett, K. E. Huber, H. Hargarten, M. H. Pespeni, Rare genetic variation and balanced polymorphisms are important for survival in global change conditions. *Proc. Biol. Sci.* **286**, 20190943 (2019).
5. M. H. Pespeni, D. A. Garfield, M. K. Manier, S. R. Palumbi, Genome-wide polymorphisms show unexpected targets of natural selection. *Proc. Biol. Sci.* **279**, 1412–1420 (2012).
6. M. W. Kelly, J. L. Padilla-Gamiño, G. E. Hofmann, Natural variation and the capacity to adapt to ocean acidification in the keystone sea urchin *Strongylocentrotus purpuratus*. *Glob. Change Biol.* **19**, 2536–2546 (2013).

7. J. L. Padilla-Gamiño, J. D. Gaitán-Espitia, M. W. Kelly, G. E. Hofmann, Physiological plasticity and local adaptation to elevated $p\ CO_2$ in calcareous algae: An ontogenetic and geographic approach. *Evol. Appls.* **9**, 1043–1053 (2016).
8. P. Calosi, S. Melatunan, L. M. Turner, Y. Artioli, R. L. Davidson, J. J. Byrne, M. R. Viant, S. Widdicombe, S. D. Rundle, Regional adaptation defines sensitivity to future ocean acidification. *Nat. Commun.* **8**, 13994 (2017).
9. H. G. Dam, J. A. deMayo, G. Park, L. Norton, X. He, M. B. Finiguerra, H. Baumann, R. S. Brennan, M. H. Pespeni, Rapid, but limited, zooplankton adaptation to simultaneous warming and acidification. *Nat. Clim. Chang.* **11**, 780–786 (2021).
10. P. Chen, J. Zhang, Antagonistic pleiotropy conceals molecular adaptations in changing environments. *Nat. Ecol. Evol.* **4**, 461–469 (2020).
11. G. L. Brennan, N. Colegrave, S. Collins, Evolutionary consequences of multidriver environmental change in an aquatic primary producer. *Proc. Natl. Acad. Sci.* **114**, 9930–9935 (2017).
12. N. Barghi, J. Hermisson, C. Schlötterer, Polygenic adaptation: A unifying framework to understand positive selection. *Nat. Rev. Genet.* **21**, 769–781 (2020).
13. N. Barghi, R. Tobler, V. Nolte, A. M. Jakšić, F. Mallard, K. A. Otte, M. Dolezal, T. Taus, R. Kofler, C. Schlötterer, Genetic redundancy fuels polygenic adaptation in *Drosophila*. *PLOS Biol.* **17**, e3000128 (2019).
14. T. M. Healy, R. S. Brennan, A. Whitehead, P. M. Schulte, Tolerance traits related to climate change resilience are independent and polygenic. *Glob. Change Biol.* **24**, 5348–5360 (2018).
15. R. S. Brennan, J. A. deMayo, H. G. Dam, M. Finiguerra, H. Baumann, V. Buffalo, M. H. Pespeni, Experimental evolution reveals the synergistic genomic mechanisms of adaptation to ocean warming and acidification in a marine copepod. *Proc. Natl. Acad. Sci.* **119**, e2201521119 (2022).
16. G. Brennan, S. Collins, Growth responses of a green alga to multiple environmental drivers. *Nat. Clim. Chang.* **5**, 892–897 (2015).
17. B. J. Sinclair, L. V. Ferguson, G. Salehipour-shirazi, H. A. MacMillan, Cross-tolerance and cross-talk in the cold: Relating low temperatures to desiccation and immune stress in insects. *Integr. Comp. Biol.* **53**, 545–556 (2013).
18. N. Gotcha, J. S. Terblanche, C. Nyamukondiwa, Plasticity and cross-tolerance to heterogeneous environments: Divergent stress responses co-evolved in an African fruit fly. *J. Evol. Biol.* **31**, 98–110 (2018).
19. E. Sanford, M. W. Kelly, Local adaptation in marine invertebrates. *Ann. Rev. Mar. Sci.* **3**, 509–535 (2011).
20. S. J. Bograd, R. J. Lynn, Long-term variability in the Southern California current system. *Deep-Sea Res. II: Top. Stud. Oceanogr.* **50**, 2355–2370 (2003).
21. F. Chan, J. A. Barth, C. A. Blanchette, R. H. Byrne, F. P. Chavez, O. Cheriton, R. A. Feely, G. Friederich, B. Gaylord, T. Gouhier, S. Hacker, T. M. Hill, G. E. Hofmann, M. A. McManus, B. A. Menge, K. J. Nielsen, A. D. Russell, E. Sanford, J. Sevadjian, L. Washburn, Persistent spatial structuring of coastal ocean acidification in the California current system. *Sci. Rep.* **7**, 2526 (2017).
22. M. G. Jacox, A. M. Moore, C. A. Edwards, J. Fiechter, Spatially resolved upwelling in the California current system and its connections to climate variability. *Geophys. Res. Lett.* **41**, 3189–3196 (2014).
23. K. J. Kroeker, E. Sanford, J. M. Rose, C. A. Blanchette, F. Chan, F. P. Chavez, B. Gaylord, B. Helmuth, T. M. Hill, G. E. Hofmann, M. A. McManus, B. A. Menge, K. J. Nielsen, P. T. Raimondi, A. D. Russell, L. Washburn, Interacting environmental mosaics drive geographic variation in mussel performance and predation vulnerability. *Ecol. Lett.* **19**, 771–779 (2016).
24. D. M. Checkley, J. A. Barth, Patterns and processes in the California current system. *Prog. Oceanogr.* **83**, 49–64 (2009).
25. M. H. Pespeni, E. Sanford, B. Gaylord, T. M. Hill, J. D. Hosfelt, H. K. Jaris, M. LaVigne, E. A. Lenz, A. D. Russell, M. K. Young, S. R. Palumbi, Evolutionary change during experimental ocean acidification. *Proc. Natl. Acad. Sci. U.S.A.* **110**, 6937–6942 (2013).
26. E. Sanford, M. S. Roth, G. C. Johns, J. P. Wares, G. N. Somero, Local selection and latitudinal variation in a marine predator-prey interaction. *Science* **300**, 1135–1137 (2003).
27. E. Kuo, E. Sanford, Geographic variation in the upper thermal limits of an intertidal snail: Implications for climate envelope models. *Mar. Ecol. Prog. Ser.* **388**, 137–146 (2009).
28. C. Hauri, N. Gruber, M. Vogt, S. C. Doney, R. A. Feely, Z. Lachkar, A. Leinweber, A. M. P. McDonnell, M. Munnich, G.-K. Plattner, Spatiotemporal variability and long-term trends of ocean acidification in the California current system. *Biogeosciences* **10**, 193–216 (2013).
29. S. A. Siedlecki, D. Pilcher, E. M. Howard, C. Deutsch, P. MacCready, E. L. Norton, H. Frenzel, J. Newton, R. A. Feely, S. R. Alin, T. Klinger, Coastal processes modify projections of some climate-driven stressors in the California current system. *Biogeosciences* **18**, 2871–2890 (2021).
30. E. M. Donham, L. T. Strope, S. L. Hamilton, K. J. Kroeker, Coupled changes in pH, temperature, and dissolved oxygen impact the physiology and ecology of herbivorous kelp forest grazers. *Glob. Change Biol.* **28**, 3023–3039 (2002).
31. J. A. Reynolds, J. E. Wilen, The sea urchin fishery: Harvesting, processing and the market. *Mar. Resour. Econ.* **15**, 115–126 (2000).
32. L. Rogers-Bennett, D. Okamoto, Mesocentrotus franciscanus and Strongylocentrotus *purpuratus: Biology and Ecology* (Elsevier, 2020), vol. 43, pp. 593–608.
33. R. S. Steneck, M. H. Graham, B. J. Bourque, D. Corbett, J. M. Erlandson, J. A. Estes, M. J. Tegner, Kelp forest ecosystems: Biodiversity, stability, resilience and future. *Envir. Conserv.* **29**, 436–459 (2002).
34. E. Sala, M. H. Graham, Community-wide distribution of predator–prey interaction strength in kelp forests. *Proc. Natl. Acad. Sci.* **99**, 3678–3683 (2002).
35. P. E. Moberg, R. S. Burton, Genetic heterogeneity among adult and recruit red sea urchins, *Strongylocentrotus franciscanus*. *Mar. Biol.* **136**, 773–784 (2000).
36. R. Strathmann, Length of pelagic period in echinoderms with feeding larvae from the northeast Pacific. *J. Exp. Mar. Biol. Ecol.* **34**, 23–27 (1978).
37. M. Pozo Buil, M. G. Jacox, J. Fiechter, M. A. Alexander, S. J. Bograd, E. N. Curchitser, C. A. Edwards, R. R. Rykaczewski, C. A. Stock, A dynamically downscaled ensemble of future projections for the California Current System. *Front. Mar. Sci.* **8**, 612874 (2021).
38. A. Bush, K. Mokany, R. Catullo, A. Hoffmann, V. Kellermann, C. Sgrò, S. McEvey, S. Ferrier, Incorporating evolutionary adaptation in species distribution modelling reduces projected vulnerability to climate change. *Ecol. Lett.* **19**, 1468–1478 (2016).
39. M. H. Pespeni, B. T. Barney, S. R. Palumbi, Differences in the regulation of growth and biomineralization genes revealed through long-term common-garden acclimation and experimental genomics in the purple sea urchin. *Evolution* **67**, 1901–1914 (2013).
40. A. R. Villeneuve, L. M. Komoroske, B. S. Cheng, Diminished warming tolerance and plasticity in low-latitude populations of a marine gastropod. *Conserv. Physiol.* **9**, coab039 (2021).
41. D. O. Conover, Seasonality and the scheduling of life history at different latitudes. *J. Fish Biol.* **41**, 161–178 (1992).
42. J. D. Arendt, Adaptive intrinsic growth rates: An integration across taxa. *Q. Rev. Biol.* **72**, 149–177 (1997).
43. S. A. Arnott, S. Chiba, D. O. Conover, Evolution of intrinsic growth rate: Metabolic costs drive trade-offs between growth and swimming performance in *Menidia menidia*. *Evolution* **60**, 1269–1278 (2006).
44. S. M. Sogard, Size-selective mortality in the juvenile stage of teleost fishes: A review. *Bull. Mar. Sci.* **60**, 1129–1157 (1997).
45. J. T. Claisse, J. P. Williams, T. Ford, D. J. Pondella, B. Meux, L. Protopapadakis, Kelp forest habitat restoration has the potential to increase sea urchin gonad biomass. *Ecosphere* **4**, 38 (2013).
46. L. Rogers-Bennett, C. A. Catton, Marine heat wave and multiple stressors tip bull kelp forest to sea urchin barrens. *Sci. Rep.* **9**, 15050 (2019).
47. R. Morgan, A. H. Andreassen, E. R. Åsheim, M. H. Finnøen, G. Dresler, T. Brembu, A. Loh, J. J. Miest, F. Jutfelt, Reduced physiological plasticity in a fish adapted to stable temperatures. *Proc. Natl. Acad. Sci.* **119**, e2201919119 (2022).
48. A. C. Vinton, S. J. L. Gascoigne, I. Sepil, R. Salguero-Gómez, Plasticity's role in adaptive evolution depends on environmental change components. *Trends Ecol. Evol.* **37**, 1067–1078 (2022).
49. C. A. Deutsch, J. J. Tewksbury, R. B. Huey, K. S. Sheldon, C. K. Ghalambor, D. C. Haak, P. R. Martin, Impacts of climate warming on terrestrial ectotherms across latitude. *Proc. Natl. Acad. Sci.* **105**, 6668–6672 (2008).
50. M. L. Pinsky, B. Worm, M. J. Fogarty, J. L. Sarmiento, S. A. Levin, Marine taxa track local climate velocities. *Science* **341**, 1239–1242 (2013).
51. M. A. Coleman, A. J. P. Minne, S. Vranken, T. Wernberg, Genetic tropicalisation following a marine heatwave. *Sci. Rep.* **10**, 12726 (2020).
52. K. J. Kroeker, R. L. Kordas, R. Crim, I. E. Hendriks, L. Ramajo, G. S. Singh, C. M. Duarte, J. -P. Gattuso, Impacts of ocean acidification on marine organisms: Quantifying sensitivities and interaction with warming. *Glob. Change Biol.* **19**, 1884–1896 (2013).
53. H. K. Hirsh, K. J. Nickols, Y. Takeshita, S. B. Traiger, D. A. Mucciarone, S. Monismith, R. B. Dunbar, Drivers of biogeochemical variability in a Central California kelp forest: Implications for local amelioration of ocean acidification. *J. Geophys. Res. Oceans.* **125**, e2020JC016320 (2020).
54. P. J. Bresnahan, Y. Takeshita, T. Wirth, T. R. Martz, T. Cyronak, R. Albright, K. Wolfe, J. K. Warren, K. Mertz, Autonomous in situ calibration of ion-sensitive field effect transistor pH sensors. *Limnol. Oceanogr. Methods* **19**, 132–144 (2021).
55. T. A. DelValls, A. G. Dickson, The pH of buffers based on 2-amino-2-hydroxymethyl-1,3-propanediol ('tris') in synthetic sea water. *Deep Sea Res. Part 1 Oceanogr. Res. Pap.* **45**, 1541–1554 (1998).
56. A. G. Dickson, C. L. Sabine, J. R. Christian, *Guide to best practices for ocean CO2 measurements* (PICES, Sydney, 2007), PICES Special Publication, *3*.

57. C. Mehrbach, C. H. Culberson, J. E. Hawley, R. M. Pytkowicx, Measurement of the apparent dissociation constants of carbonic acid in seawater at atmospheric pressure. *Limnol. Oceanogr.* **18**, 897–907 (1973).
58. A. G. Dickson, F. J. Millero, A comparison of the equilibrium constants for the dissociation of carbonic acid in seawater media. *Deep Sea Res. Part 1 Oceanogr. Res. Pap.* **34**, 1733–1743 (1987).
59. S. Davies, Short-term growth measurements of corals using an accurate buoyant weighing technique. *Mar. Biol.* **101**, 389–395 (1989).
60. C. Olito, C. R. White, D. J. Marshall, D. R. Barneche, Estimating monotonic rates from biological data using local linear regression. *J.Exp. Biol.* **220**, 759–764 (2017).
61. J. F. Steffensen, P. G. Bushnell, H. Schurmann, Oxygen consumption in four species of teleosts from Greenland: No evidence of metabolic cold adaptation. *Polar Biol.* **14**, –49, 54 (1994).

Acknowledgments: We thank S. Lummis, I. Norton, and B. Walker for assistance in the field. We also thank P. Raimondi for data analysis advice; S. Myers, A. Rogers, and A. Snyder for invaluable assistance during the experiment; and N. Moore for providing facilities support for our mesocosm system. **Funding:** This work was supported by the Institute for the Study of Ecological and Evolutionary Climate Impacts Graduate Fellowship (EMD) and California Ocean Protection Council award C0302200 (to K.J.K., J.F., and Y.T.). **Author contributions:** Conceptualization: E.M.D. and K.J.K. Methodology: E.M.D., K.J.K., and Y.T. Investigation: E.M.D., I.F., A.H., E.O., and K.V. Visualization: E.M.D. Supervision: E.M.D., K.J.K., and J.F. Writing—original draft: E.M.D. and K.J.K. Writing—review and editing: E.M.D., I.F., A.H., E.O., K.V., Y.T., J.F., and K.J.K. **Competing interests:** The authors declare that they have no competing interests. **Data and materials availability:** The code and raw data that support the findings of this study are openly available in GitHub at https://github.com/EmilyDonham/UrchinPopCC, and raw data can also be found in the Dryad data repository (https://doi.org/10.7291/D1V10Q).

Submitted 5 August 2022
Accepted 20 December 2022
Published 20 January 2023
10.1126/sciadv.ade2365